ORIGINAL ARTICLE

Algorithm of Micro-Grooving and Imaging Processing for the Generation of High-Resolution Structural Color Images

Tianfeng Zhou[1] · **Yupeng He**[1] · **Tianxing Wang**[1] · **Xiaobin Dong**[1] · **Peng Liu**[1] · **Wenxiang Zhao**[1] · **Yao Hu**[2] · **Jiwang Yan**[3]

Abstract

The use of submicron structures for structural coloration of surfaces has broad applications for color filters, projection displays, virtual reality, and anti-counterfeiting. Currently, structural color images lack high resolution due to low manufacturing accuracy. In this study, the axial-feed fly cutting (AFC) method is proposed to fabricate submicron grooves for the diffraction of visible light to create structural color images. We establish the relationship between the color information in the pixels of the original image and the parameters of the array units corresponding to the pixels. An algorithm to determine groove spacing and the tool path is established, and array units with the desired groove spacing are machined to reproduce the structural color images. The submicron grooves fabricated by AFC have high quality and good consistency. Due to the excellent diffraction performance of the machined grooves, images with high saturation and resolution can be reproduced. It is verified that images with various colors can be efficiently fabricated using the proposed method and algorithm.

Keywords Submicron structure · Microgroove · Structural coloration · Structural-color image · Fly cutting · Micro-machining

1 Introduction

Structural coloration has the advantages of high brightness, no fading, and no pollution, and the method has a range of applications for color filters, displays, virtual reality, and anti-counterfeiting [1–4]. Structural coloration is not caused by chemical pigments but instead by complex interactions between visible light and the workpiece surface. The photonic mechanisms underlying structural coloration include the plasma effect, as well as diffraction, scattering, and interference [4, 5]. Diffraction-grating-induced structural coloration is a method to generate high-resolution structural color images by manufacturing submicron structures and provides a pronounced iridescent effect [6–8], causing apparent changes in the color at different viewing angles.

Submicron structure manufacturing requires high efficiency and high quality. Lithography is a traditional method for grating manufacturing and is highly efficient but limited by the surface quality of the machined microstructures. Etching technology can be used to fabricate complex structures at the nanometer scale. However, the machining process is very complicated, and the size of the workpiece is limited [9–11]. Femtosecond lasers are widely used to generate periodic submicron structures and have been successfully used to manipulate the color of the machined surface. Femtosecond lasers have high processing efficiency, but the poor accuracy and homogeneity of the machined microstructure result in color dispersion, which decreases the resolution of the structural color images [12–14].

Mechanical cutting methods using diamond tools are suitable for generating submicron-scale structures. Guo and Yang used ultrasonic vibration in a microstructure machining process to produce an elliptical vibration of the diamond tool and achieve high-efficient fabrication of submicron strips [15, 16].

✉ Tianfeng Zhou
zhoutf@bit.edu.cn

1   Key Laboratory of Fundamental Science for Advanced Machining, Beijing Institute of Technology, Beijing 100081, China

2   Beijing Key Laboratory for Precision Optoelectronic Measurement Instrument and Technology, Beijing Institute of Technology, Beijing 100081, China

3   Department of Mechanical Engineering, Faculty of Science and Technology, Keio University, Yokohama 223-8522, Japan

Strip spacing is a crucial parameter in the optical manipulation and is adjusted by changing the feed rate of the cutting tool in elliptical vibration cutting (EVT). Submicron strips with different spacings were produced by EVT to create colorful images. However, the accuracy of the machined submicron structures was low, and the boundaries between the adjacent structures were deformed, which caused strong light dispersion and reduced the color resolution of the structural coloration images. Therefore, a new machining method is needed to improve the accuracy of the submicron structures and obtain high-resolution images. In addition, challenges remain regarding submicron-structure manufacturing and methods for creating structural color images [17–19].

In conventional fly cutting, the features in the workpiece are fabricated by feeding the workpiece in the radial direction of the spindle; a single groove is fabricated in each step, and multiple cutting steps are required, resulting in low efficiency. In this paper, we propose a mechanical cutting method called axial-feed fly cutting (AFC) to fabricate submicron structures for creating structural color images. During the AFC process, submicron optical grooves are fabricated and arrayed using a cutter with high-speed rotation and feeding the workpiece in the direction of the spindle axis. Diffraction grating is used, and an algorithm is established based on the relationship between the pixel information and the parameters of the array units. Process planning is used to fabricate and align array units with color information; this configuration allows for the generation of large, high-resolution images with excellent color reproduction. The proposed cutting method provides high accuracy of the submicron structures for structural coloration, as well as high-efficiency reproduction of high-resolution images. The machined image on the workpiece surface accurately reproduces the original high-resolution image, demonstrating that AFC is suitable for structural coloration and is capable of high-resolution image production.

We investigate the principle of structural coloration induced by submicron optical grooves. Before fabricating the structural-color image, image processing is conducted to determine the relationship between the pixel information and the parameters of the array unit, and process planning is performed for image reproduction. Experiments are conducted to verify the feasibility of the AFC method for structural coloration. Subsequently, the proposed AFC method and image processing algorithm are successfully used for the creation of high-resolution images.

2 Surface Machining Using Fly Cutting

2.1 Periodic Submicron Grooves Created by Fly Cutting

The structural coloration is created by the submicron structure array, which has the same scale as that of the wavelength of visible light. Fly cutting has the advantages of simple operation, high efficiency, and high processing quality for microstructure manufacturing [20, 21]. We proposed the AFC method for efficient manufacturing and flexible control of the microstructure. Figure 1 shows the schematic diagram of the AFC method. A 90° V-shaped diamond cutting tool is attached to a high-speed rotating spindle; the rake face of the tool is perpendicular to the rotation direction of the fly cutting process, and the workpiece is fed in the direction of the spindle axis (Z-axis). One groove is generated per rotation of the cutting tool, and the grooves are arrayed while the workpiece is fed perpendicular to the rotation plane of the cutting tool. Instead of removing the material step-by-step to reduce the cutting volume and improve the processing quality in traditional fly cutting, in the AFC method, the tool rotates at high speeds to generate a groove in a single rotation. The high cutting speed of the fly-cutting process allows for high-efficiency manufacturing of submicron structures while ensuring excellent quality.

During the AFC process, the radius of rotation of the tool tip is within tens of millimeters, which is far greater than the cutting depth of the submicron grooves. During a single rotation of the cutting tool, one groove is machined rapidly; therefore, the effects of feeding the workpiece on the morphology of the grooves can be ignored. One groove is generated on the surface during a single rotation of the
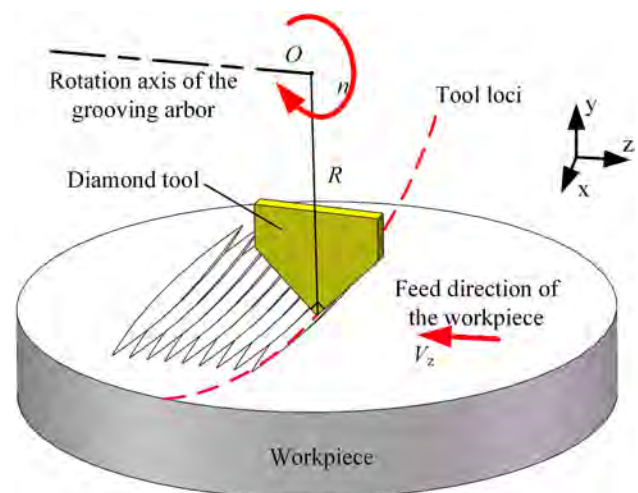

Fig. 1 Schematic diagram of the AFC method

spindle, as shown in Fig. 2a. This groove has a very large aspect ratio, and the depth of the groove increases from 0 on both ends to the maximum in the middle. It can be learnt that the cross-section profile of the machined submicron groove is consistent with the projection of blade tip on base surface during machining, which means the groove shape can be regulated by the tool geometry.

When the workpiece is fed in the direction of the spindle axis while the cutting tool rotates, parallel grooves are generated. Figure 2b shows the schematic diagram of the grooves on the surface of the workpiece generated by AFC. The groove spacing is defined as the distance between the centers of adjacent grooves, which is determined by the feed rate when the spindle speed is fixed during machining. Parallel submicron grooves are produced similar to those created by diffraction grating. The groove spacing is adjusted to achieve coherent diffraction of light for structural coloration. On both sides of the structure, the distance between the grooves differs from that in the middle of the grooves because the cutting depth is low at the groove tips, which increases the dispersion of the diffracted light and reduces the diffraction efficiency and resolution. Therefore, the groove tips should be removed when high-resolution images are desired.

In AFC, when the tool speed is given, the slower the workpiece feed speed, the denser the submicron grooves are, and the smaller the groove spacing is. The groove spacing (d) has the following relationship with the rotation speed of the tool (n) and the feed rate (V_z) of the workpiece in the spindle-axis direction:

$$d = \frac{V_z}{n} \tag{1}$$

For example, at a tool rotation speed of 4500 rpm and a feed rate of 4.5 μm/min, the groove spacing is 100 nm. The submicron groove spacing can be adjusted in a wide range by setting a reasonable tool rotation speed and feed rate parameters during processing. During the operation, it is more convenient to adjust the feed rate and keep the rotation speed of the tool constant, which allows for flexible control of the groove spacing. Since the grooves have the same scale as the wavelength of visible light, the AFC method to create submicron grooves represents an advance in surface manufacturing for structural coloration.

2.2 Principle of Generating the Surface

The diffraction of the visible light resulting from the submicron-scale groove size is the underlying mechanism of structural coloration. Interference occurs when the light is diffracted from different grooves, enhancing the intensity of the diffracted light where the multiple diffracted light has the same phase. Similar to diffractive grating, the submicron grooves with submicron spacing produce iridescent structural color, as shown in Fig. 3.

The relationship between the grating spacing and the angles of the incident and diffracted beams of light is defined in the grating equation:

$$d(\sin \theta_i + \sin \theta_m) = m\lambda \quad m = (0, \pm1, \pm2, \ldots) \tag{2}$$

where d is the groove spacing, θ_i is the incident angle, θ_m is the diffraction angle (the viewing angle). λ and m are the wavelength and diffraction order of the diffracted light, respectively. When beams of parallel white light are incident on the surface with submicron grooves, iridescent color is observed at different viewing angles. The light wavelength λ of the corresponding color is defined as:

$$\lambda = \frac{d(\sin \theta_i + \sin \theta_m)}{m} \tag{3}$$

The intensity of the diffracted light decreases with increasing diffraction order, and the maximum intensity occurs at the first diffraction order [22]. When the observation angle (θ_m) is given, the diffraction wavelength is determined by the angle of incidence (θ_i) and the groove spacing.

$$\lambda = d(\sin \theta_i + \sin \theta_m) \tag{4}$$

Fig. 2 Periodic submicron grooves obtained by AFC. **a** Single groove. **b** Parallel grooves
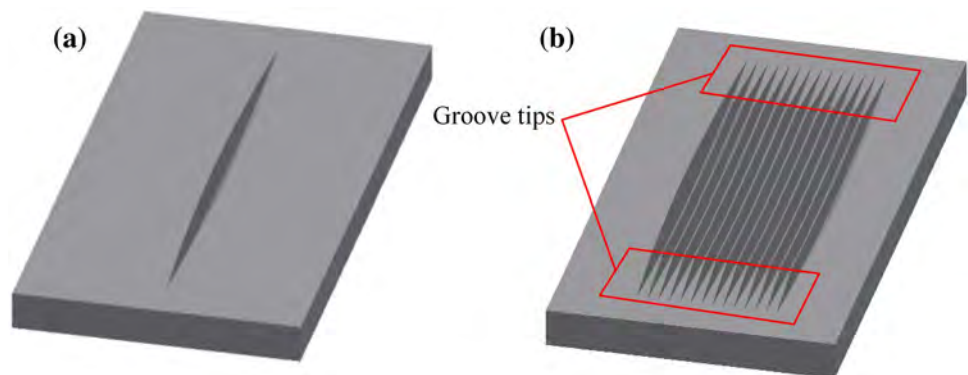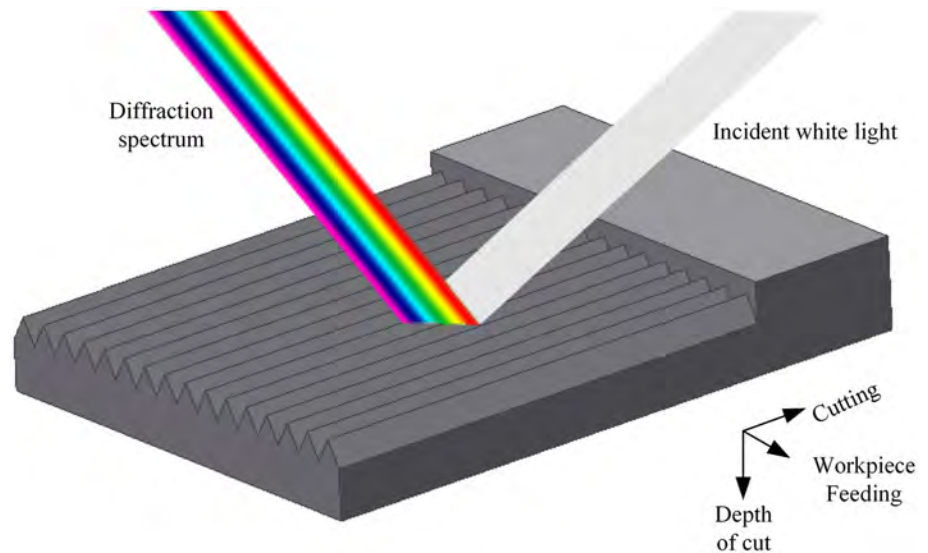
Groove tips

Fig. 3 Schematic of structural coloration caused by the grooves

If white light is incident in a direction perpendicular to the surface ($\theta_i = 0$), the diffracted wavelengths obtained at different viewing angles are determined as follows:

$$\lambda = d \sin \theta_m \tag{5}$$

According to Eq. (5), all diffraction colors with wavelengths shorter than the current groove spacing in the spectrum can be obtained by adjusting the viewing angle. In addition, according to grating diffraction theory, when the groove spacing is close to the wavelength of visible light, the intensity of the diffracted light is high at all wavelengths. Therefore, the groove spacing is set to the wavelength of the diffracted light of the target color in the structural coloration design to improve the iridescent effect as follows:

$$\lambda = d \tag{6}$$

According to Eq. (6), at the same incident angle and viewing angle, grooves with a large spacing diffract light with a long wavelength. The target structural color is only determined by the submicron groove spacing (d) instead of the groove shape, and the groove spacing can be flexibly regulated by the feed rate in the VFC process. A small groove produces structural color with a short wavelength.

According to diffraction theory, an array unit with particular submicron groove spacing will produce structural color in a particular wavelength. Therefore, the surface can be machined using array units with different spacings, as illustrated in Fig. 4, and the groove spacing is determined by the feed rate of the AFC method. This real-time regulation of the feed rate in AFC allows for flexible manipulation of the groove spacing, thereby improving the manufacturing accuracy of the surface used for structural coloration.
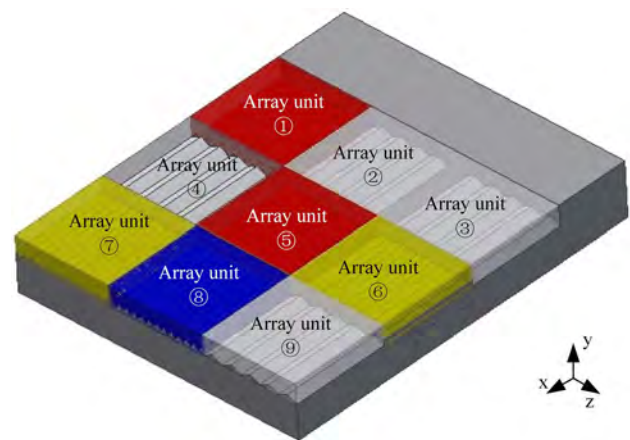
Fig. 4 Structural coloration method to reproduce color using array units

3 Algorithm for Image Reproduction

3.1 Image Processing

An image consists of pixels and can be considered a pixel matrix. The color information of the image is stored in the pixels. To reproduce structural-color images, an array unit with particular groove spacing is used as the pixel unit. The image reproduction process on a workpiece consists of converting color information of pixels into the corresponding diffraction wavelength; subsequently, then the groove spacing is obtained based on the target diffraction wavelength and is used during the manufacturing of the array unit.

The pixel color is described using a color model, and the information is stored in a numerical matrix. The red,

green, and blue (RGB) color model is a common color model and is widely used in digital images. In the RGB model, the red, green, and blue light is combined to obtain various colors. The RGB model is advantageous and convenient for computer processing and recording. However, it is difficult to convert a three-dimensional matrix to the one-dimensional wavelength to achieve the correct groove spacing. Therefore, the hue, saturation, and value (HSV) model, which is also a three-dimensional color model, is used in image processing to convert the color information. In the HSV color space, the color information is described by the hue axis instead of three axes. Therefore, the hue of the HSV space is used to convert the color of the original image to the corresponding wavelength and groove spacing.

First, the colors of the original image in the RGB model are converted to the hue values of the HSV model as follows:

$$h = \begin{cases} 0° & \text{if max} = \text{min} \\ 60° \times \frac{g-b}{\text{max}-\text{min}} + 0° & \text{if max} = r \text{ and } g \geq b \\ 60° \times \frac{g-b}{\text{max}-\text{min}} + 360° & \text{if max} = r \text{ and } g < b \\ 60° \times \frac{b-r}{\text{max}-\text{min}} + 120° & \text{if max} = g \\ 60° \times \frac{r-g}{\text{max}-\text{min}} + 240° & \text{if max} = b \end{cases} \quad (7)$$

The color distribution on the hue axis is similar to that of the visible spectrum. The hue axis is a circular axis, where purple is adjacent to red. The range of the normalized hue is 0–1, and the wavelength range of the visible spectrum is 0.41–0.71 μm. Second, function fitting is used to convert the obtained hue value into the wavelength using MATLAB. The following calibrated linear transfer function is used to associate the hue with the wavelength:

$$\lambda = \begin{cases} -0.26 \times h + 0.64 & h \in [0, 0.9) \\ 0.70 \times h + 0.01 & h \in [0.9, 1] \end{cases} \quad (8)$$

Third, calibration is conducted by extracting the hue of the captured diffracted color and mapping it to the wavelength given by Eq. (5). According to Eq. (6), the diffraction wavelength is the same as the submicron groove spacing; therefore, the groove spacing is obtained. Image processing, including color model transformation and extraction of the hue value, are conducted in MATLAB; the process is illustrated in Fig. 5.

Black and white are not included on the hue axis, which means wavelengths cannot be used to describe these colors. Black is obtained by combining the primary colors. According to Eq. (2), black in the structural coloration can be obtained by reducing the groove spacing to the ultraviolet spectrum, which weakens the diffracted visible light after interference. Similarly, when the groove spacing is much larger than the visible light wavelength, no iridescence will occur, and the color of the workpiece will be nearly white. According to the processing quality and the desired structural color, the groove spacings for white and black in the structural coloration are set to 3000 and 200 nm, respectively. Because there is no black and white on the hue axis, the black and white colors of the original image are converted to gray values instead of the hue value.

Theoretically, the proposed AFC method can be used to fabricate images with no resolution limit. A higher resolution of the target image means that there are more pixels per unit area on the surface and smaller grooves, resulting in increased processing time for reproducing high-resolution images. Therefore, the resolution of the target image needs to be as high as possible to ensure good image quality while minimizing the processing time. The optimization of this process is performed using the imaging editing software Adobe Photoshop (Adobe Inc.).

3.2 Tool Path Planning

The target image is divided into a pixel matrix, where every pixel corresponds to an array unit on the machined surface. Therefore, the goal of achieving high-resolution image reproduction is equivalent to generating a matrix composed of array units with the corresponding groove spacing.

The reproduction of the image is performed pixel-by-pixel, where each pixel corresponds to an array unit with a particular spacing. Since each pixel has only one color value corresponding to a particular groove spacing, and the groove spacing is determined by the feed rate, the feed rate of the workpiece remains constant during the manufacturing of one array unit. The feed rate changes to another constant value when another unit is machined. Therefore, tool path planning is conducted to convert the color information of each pixel to the feed rate using the proposed algorithm. The coordinate of the array unit is output and changed to G code for the machine tool. It should be noted that there is a ratio between the size of the original image and that of the machined image, which means the coordinate transformation from the original pixel has to consider this ratio.

For an original pixel matrix (3 × 3) (Fig. 6a), one row of array units is fabricated in one Z-axis feed. The feed rate changes during the fabrication, resulting in a step curve of the feed rate, as shown in Fig. 6b. Moreover, the step width of the feed rate is equal to the size of the machined array unit and pixel. After one row of array units has been machined, the rotating fly-cutting tool returns to the start position (non-cutting path) before machining the next row of array units; this process minimizes errors resulting from tool lifting, as shown in Fig. 6b. The rows of array units are machined using the same feed trajectory.

As discussed, the tips of the submicron grooves should be removed before producing the structural coloration images.

Fig. 5 Image processing for the generation of structural color images
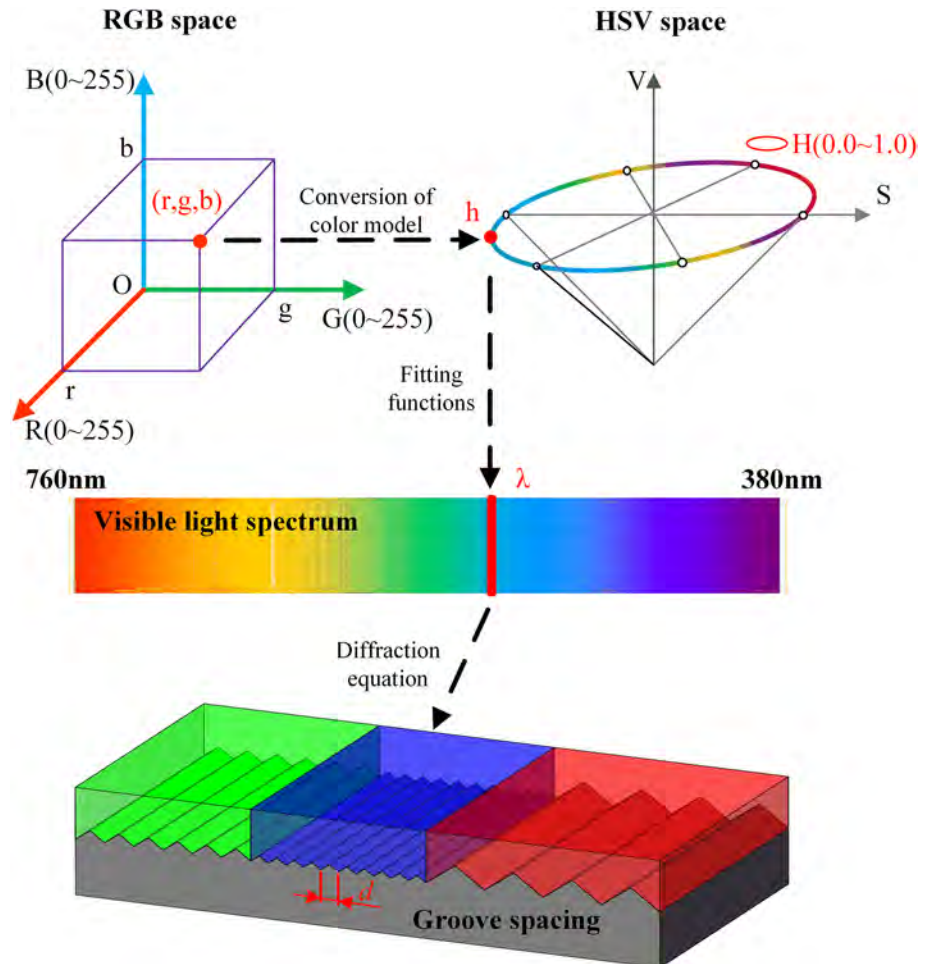
Since the pixel size is far smaller than the groove length, the previous row of groove tips is removed during the fabrication of the next row of grooves. After machining, the pixel information and the resolution are inherent in the groove spacing of the array unit. The feed rate in AFC is automatically planned and executed by the program; therefore, it is possible to produce high-resolution images with various colors using the AFC method.

4 Experimental Verification

4.1 Experimental Setup and Details

Since the material removal during the manufacturing of the submicron grooves occurs at the submicron level, the fabrication requires a sufficiently high spindle speed and accurate feed motion in the Z-axis direction. Therefore, the stability and accuracy of the machine platform have to be high. The platform used for the AFC method is the ultra-precision machine Nanoform X (produced by Precitech Corporation, USA), as shown in Fig. 7. The tool is attached to the spindle

to achieve high-speed rotation, and the maximum rotation speed is 10,000 rpm. The peak-to-valley (P–V) value of the dynamic balance is adjusted to less than 10 nm using the balance system of the ultra-precision platform. The X-axis and Z-axis are the two moving axes, with a maximum stroke of 220 mm and a maximum feed rate of 4000 mm/min, which meets the processing requirements. During processing, a single row of array units of the target image is machined by feeding the workpiece in the Z-axis direction, and row-by-row processing of the array units is performed by feeding the workpiece in the X-axis direction. The accuracy in the Z-axis direction of the machine platform is 0.1 μm/50 mm, and the resolution accuracy is 0.1 nm, resulting in accurate positioning of the array units. In addition, the granite base and TMC MaxDamp damping device of the ultra-precision machine ensures stability during machining.

The workpiece material consisted of stainless steel with a nickel phosphide (Ni–P) coating applied using electroless plating. Electroless Ni–P coating has high strength and hardness and good performance for micro/nano-scale machining [23–27]. The nominal diameter of the stainless steel is 13 mm, and the thickness of the Ni–P coating is 200 μm.
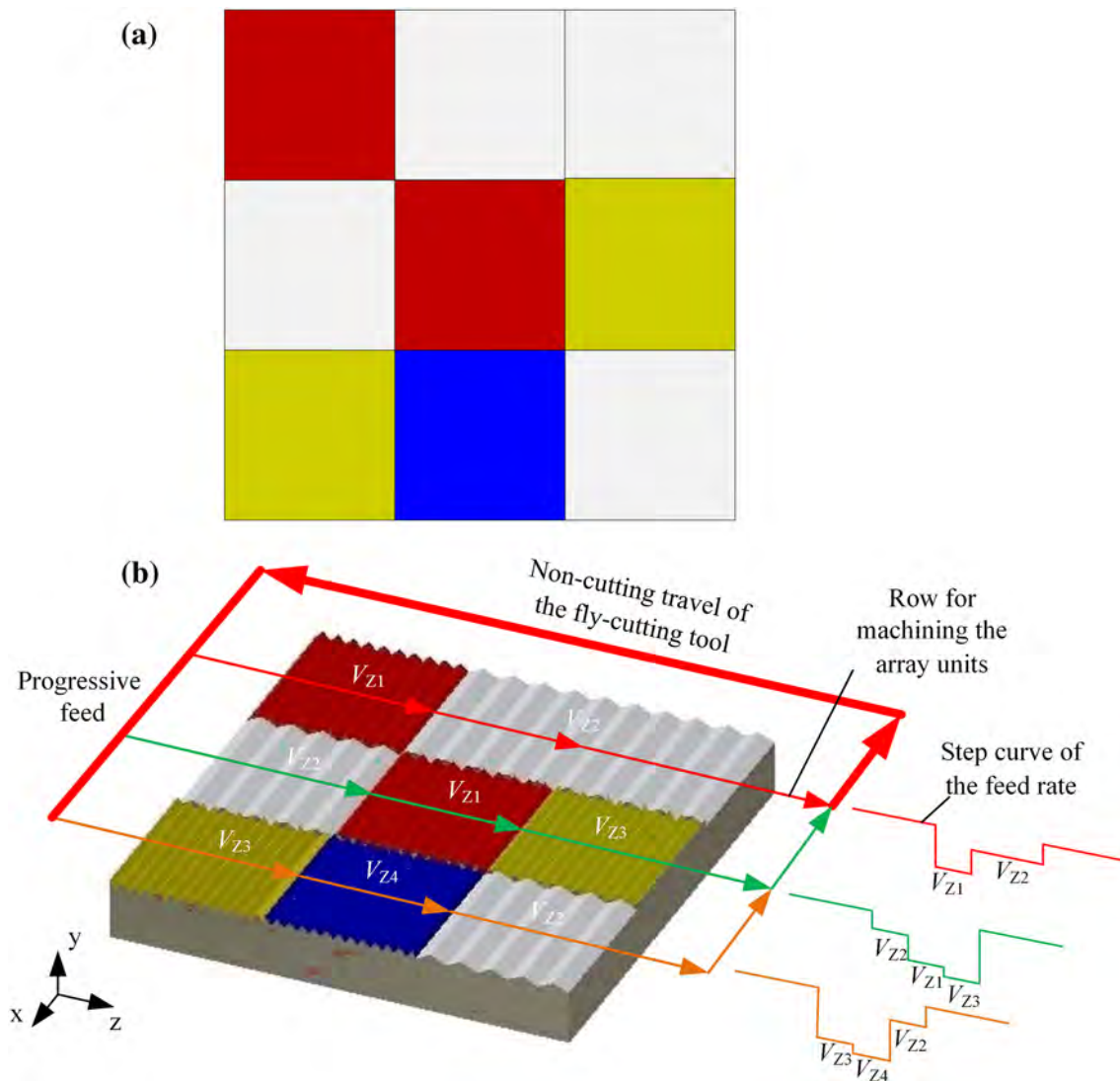
Fig. 6 Tool path planning for machining the pixel matrix. **a** 3 × 3 pixel matrix. **b** Machining of the 3 × 3 array unit matrix

The Ni–P workpiece was clamped on the workbench. The 90° V-shaped single-point diamond tool with rake angle of 0 and clearance angle of 12° was installed on the grooving arbor in the radial direction; the tool has a low affinity with non-ferrous metals and excellent mechanical properties. The vertical position tolerance of the workpiece surface should be within 100 nm; therefore, the workpiece was flattened before structural coloration processing. Flattening was conducted using conventional fly cutting technology and an R5 arc diamond tool. The surface roughness of the workpiece was within 10 nm.

The positioning stage, which has a piezoelectric drive and a frictionless flexible guiding structure, was used to adjust the cutting depth and vertical positioning; this configuration has the advantages of a large load, large displacement, and high precision. The nominal stroke was 95 μm, and the

position resolution was 10 nm, which met the high precision and rapid positioning requirements of the tool for structural coloration processing.

The spindle speed was 4500 rpm to ensure spindle stability and processing efficiency. As discussed above, the groove period used in the manufacturing process was in the visible spectrum (380-760 nm). The experimental results of using the AFC method for the fabrication of the submicron grooves are shown in Fig. 8. Grooves with a spacing of 1000 nm and 100 nm were fabricated with feed rates of 4.5 mm/min and 0.45 mm/min, as shown in Fig. 8a, b, respectively. It is observed that the grooves machined with a 4.5 mm/min feed rate have a spacing that is similar to the designed value of 1000 nm, and the grooves have high consistency and are parallel. No defects are observed. The grooves machined with a 0.45 mm/min feed rate have

Fig. 7 AFC platform for structural-color image manufacturing. **a** Installation diagram of the AFC platform and **b** photograph of the AFC platform
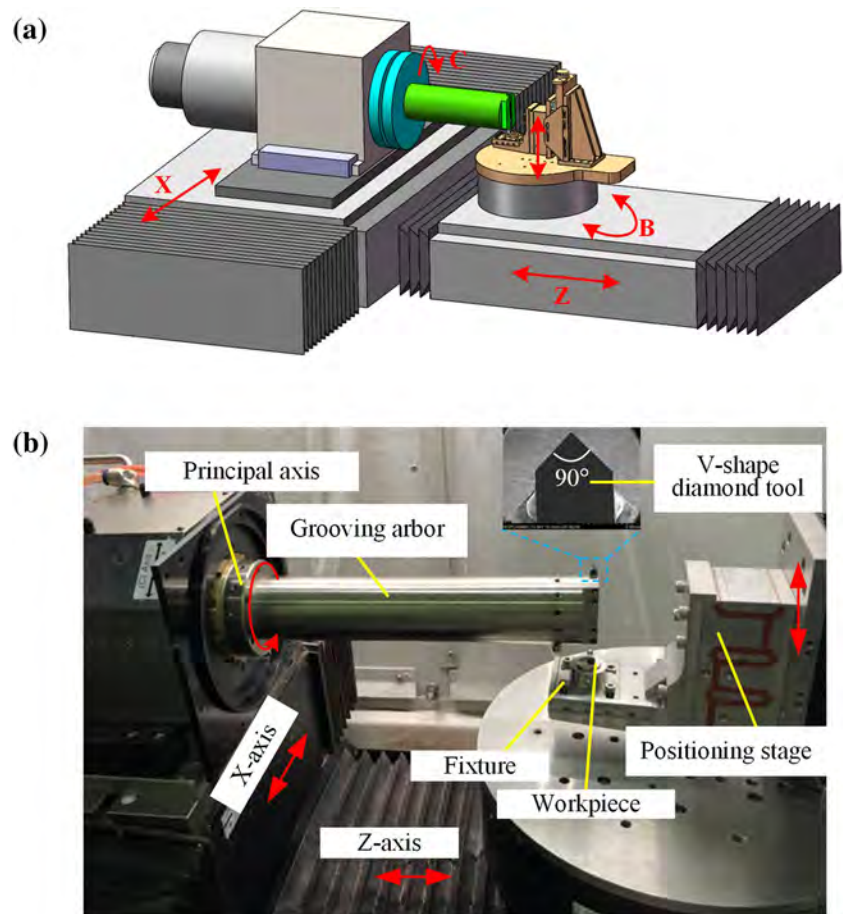
a period of approximately 100 nm, which is the same as the designed value. As mentioned before, the advantage of image reproduction by AFC is the ability to control the feed rate during the machining process. The feed rate was changed from 9 mm/min to 1.35 mm/min (with a groove spacing of 2000 nm and 300 nm, respectively) to assess the effect of changing the feed rate, as shown in Fig. 8c, d. It is observed that a change in the feed rate does not affect the groove spacing; the grooves with different spacing exhibit good consistency, and only one or two grooves show differences in the spacing. These results verify that the proposed AFC method is well suited for high-efficiency fabrication of submicron grooves; the ultra-precision machining platform meets the requirements for the reconstruction of images using structural coloration.

4.2 Fabrication of High-Resolution Images

The proposed AFC method was used to create structural color images. As shown in Fig. 9, the original image (Fig. 9a) is accurately duplicated, and structural color images are created on the Ni–P coating (Fig. 9b). The original colorful image is divided into a 158 × 158 pixel matrix, which means that the machined array units all have the same size of 85.4 μm × 85.4 μm after being machined on the surface with a diameter of 13.5 mm. Spindle speed of 4500 rpm is fixed and the feed rate corresponding to the groove spacing is changed according to the target color during the machining process. The total processing time of the image shown in Fig. 9b is about 363 min. Iridescence is observed on the grooved surface under natural light. A white light from a mobile flashlight (iPhone 6s) illuminates on the machined surface. The cartoon image "Angry Bird" is shown under a white light with an incident angle of 0°, and an image is acquired with a digital camera. The photograph shows that the structural color images have high color saturation, bright colors, high resolution, and a clear outline. The results verify the feasibility of using the AFC method to generate submicron grooves and obtain structural color images with high resolution.

The proposed algorithm that combines image processing and tool path planning can be used theoretically to reproduce images of any color on a surface using AFC. The grooves produced by AFC have high diffraction for visible light and high manufacturing efficiency of structural color images.
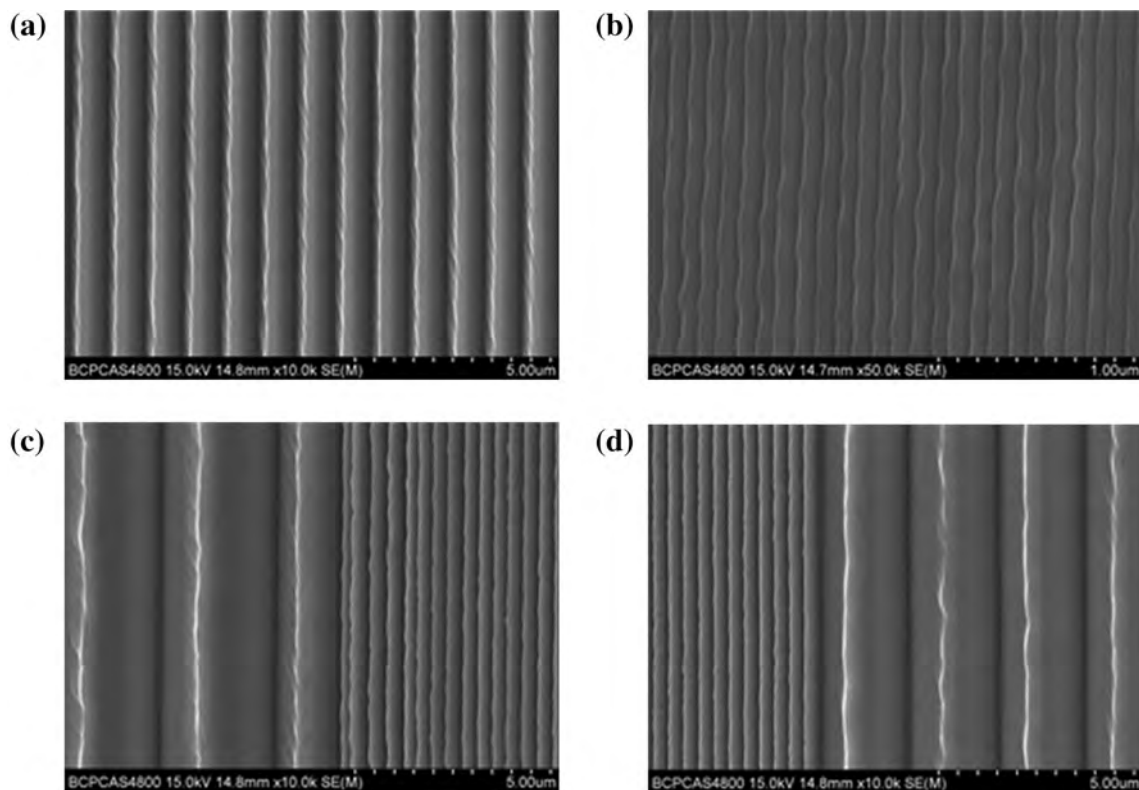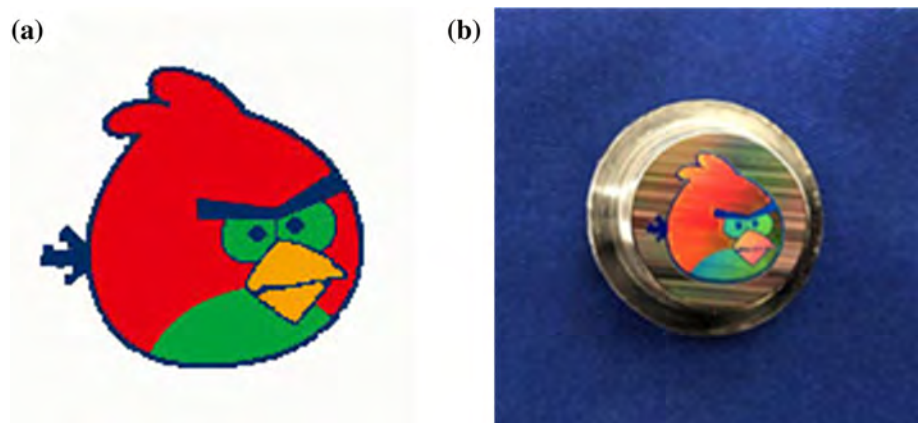
Fig. 8 Machined submicron grooves: grooves machined with a feed rate of **a** 4.5 mm/min and **b** 0.45 mm/min; change in the feed rate from **c** 9 mm/min to 1.35 mm/min and **d** from 1.35 mm/min to 9 mm/min

Fig. 9 High-resolution structural color images created with the AFC method. **a** Original images. **b** Structural color images

5 Conclusions

We proposed the AFC method to fabricate submicron optical structures for structural coloration. Theoretical analysis was conducted, and the proposed method consisting of image processing and tool path planning was used to reproduce high-resolution structural color images on Ni–P coating. The main conclusions are as follows:

1. AFC proved highly suitable for manufacturing submicron optical structures with high efficiency. The desired colors of the images are determined by the groove spacing, which was controlled by adjusting the machining parameters.

2. An algorithm was developed to convert the pixel information into the required spacing of the grooves of the array units. The RGB information of the original image

was converted to the hue value, and a linear transfer function was used to determine the corresponding groove spacing.

3   The array units were arranged side-by-side to ensure a parallel feed trajectory of the workpiece, and high-resolution images with high-saturation colors were reproduced.

The resulting high-resolution images demonstrated that the submicron structures fabricated using the AFC method provided good color rendering. The proposed method has potential applications in the fields of micro-optics, anti-counterfeiting, and displays.

Availability of data and material Materials and data described in the manuscript will be freely available to any scientist wishing to use them for non-commercial purposes, without breaching participant confidentiality.
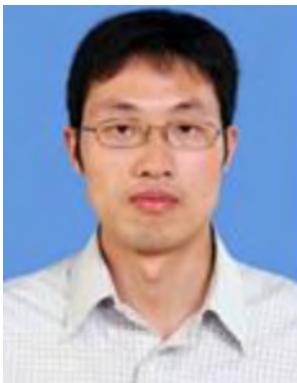
Compliance with Ethical Standards

Conflict of interest The authors declare that they have no conflict of interest.

References

1. Chu L, Zhang X, Niu W, Wu S, Ma W, Tang B, Zhang S (2019) Hollow silica opals/cellulose acetate nanocomposite films with structural color for anti-counterfeiting of banknotes. J Mater Chem C. https://doi.org/10.1039/C9TC01992H

2. Li H, Sun X, Peng H (2015) Mechanochromic fibers with structural color. ChemPhysChem 16(18):3761–3768. https://doi.org/10.1002/cphc.201500736

3. Arsenault A (2012) Opalux photonic ink: full-color, bistable, reflective displays. APS March meeting 2012 American Physical Society

4. Engl G, Kolle M, Kim P, Khan M, Muñoz P, Mazur E, Aizenberg J (2014) Bioinspired micrograting arrays mimicking the reverse color diffraction elements evolved by the butterfly pierella luna. Proc Natl Acad Sci USA 111(44):15630. https://doi.org/10.1073/pnas.1412240111

5. Proietti Zaccaria R (2016) Butterfly wing color: a photonic crystal demonstration. Opt Lasers Eng. https://doi.org/10.1016/j.optlaseng.2015.04.008

6. Sun J, Bhushan B, Tong J (2013) Structural coloration in nature. RSC Adv 3(35):14862. https://doi.org/10.1039/c3ra41096j

7. Lindsey DT (2000) Vision science: photons to phenomenology. Vis Sci 77(4):233–234. https://doi.org/10.1097/00006324-200005000-00008

8. Chowdhury D, Paul A, Chattopadhyay A (2001) Patterning design in color at the submicron scale. Nano Lett 1(8):409–412. https://doi.org/10.1021/nl0155678

9. Huang M, Yeh S, Lee C-K, Huang T (1996) Large-format grating image hologram based on e-beam lithography. Pract Hologr X. https://doi.org/10.1117/12.236052

10. Liu Z, Pan C, Chao C-H, Wang W, Liu CY (2013) Fabrication of high-verticality grating nanostructures using twice-deposited etching mask layers. J Nano Res 25:145–156. https://doi.org/10.4028/www.scientific.net/JNanoR.23.24

11. Chen C G, Konkola P T, Heilmann R K, Joo C, Schattenburg M L (2002) Nanometer-accurate grating fabrication with scanning beam interference lithography. In: Spies international symposium on smart materials. International Society for Optics and Photonics. https://doi.org/10.1117/12.469431

12. Son Y, Yeo J, Moon H, Lim TW, Hong S, Nam KH, Yoo S, Grigoropoulos CP, Yang DY, Ko SH (2011) Nanoscale electronics: digital fabrication by direct femtosecond laser processing of metal nanoparticles. Adv Mater 23(28):3176–3181. https://doi.org/10.1002/adma.201100717

13. Li Y, Bai F, Fan W, Zhao Q (2016) Color difference analysis of femtosecond laser colorized metals. Acta Opt Sin 36(7):0714003. https://doi.org/10.3788/AOS201636.0714003

14. Ionin AA, Kudryashov SI, Makarov SV, Seleznev LV, Sinitsyn DV, Golosov EV, Golosova OA, Kolobov YR, Ligachev AE (2012) Femtosecond laser color marking of metal and semiconductor surfaces. Appl Phys A Mater Sci Process A107(2):301–305. https://doi.org/10.1007/s00339-012-6849-y

15. Yang Y, Pan Y, Guo P (2017) Structural coloration of metallic surfaces with micro/nano-structures induced by elliptical vibration texturing. Appl Surf Sci 402(Complete):400–409. https://doi.org/10.1016/j.apsusc.2017.01.026

16. Yang Y, Guo P (2019) Global tool path optimization of high-resolution image reproduction in ultrasonic modulation cutting for structural coloration. Int J Mach Tools Manuf 138:14–26. https://doi.org/10.1016/j.ijmachtools.2018.11.002

17. Huang R, Zhang X, Neo WK, Kumar AS, Liu K (2018) Ultra-precision machining of grayscale pixelated micro images on metal surface. Precis Eng. https://doi.org/10.1016/j.precisioneng.2017.12.009

18. Kampherbeek BJ, Wieland MJ, Kruit P (2000) Resolution of the multiple aperture pixel by pixel enhancement of resolution electron lithography concept. J Vac Sci Technol B Microelectron Nanom Struct 18(1):117–121. https://doi.org/10.1116/1.591161

19. Wang P, Liu DL, Liu YZ, Liu XL, Wu CY (2008) PCBN tool performance evaluation based on image analysis of machining surface texture. Appl Mech Mater 10–12:762–766. https://doi.org/10.4028/www.scientific.net/AMM.10-12.762

20. Dong X, Zhou T, Pang S, Liang Z, Ruan B, Zhu Z, Wang X (2018) Mechanism of burr accumulation and fracture pit formation in ultraprecision microgroove fly cutting of crystalline nickel phosphorus. J Micromech Microeng. https://doi.org/10.1088/1361-6439/aae8f9

21. Steinkopf R, Scheiding S, Gebhardt A, Risse S, Eberhardt R, Tünnermann A (2012) Fly-cutting and testing of freeform optics with sub-μm shape deviations. Curr Dev Lens Des Opt Eng XIII. https://doi.org/10.1117/12.928963

22. Ou Z, Huang M, Zhao F (2014) Colorizing pure copper surface by ultrafast laser-induced near-subwavelength ripples. Opt Express 22(14):17254–17265. https://doi.org/10.1364/oe.22.017254

23. Yan J, Sasaki T, Tamaki J, Kubo A, Sugino T (2004) Chip formation behaviour in ultra-precision cutting of electroless nickel

plated mold substrates. Key Eng Mater 257–258:3–8. https://doi.org/10.4028/www.scientific.net/KEM.257-258.3

24. Zhou T, Yan J, Kuriyagawa T (2012) Size effects on transferability and mold change of glass molding press for microgrooves. Adv Mater Res 497:235–239. https://doi.org/10.4028/www.scientific.net/AMR.497.235

25. Yu Q, Zhou T, Jiang Y, Yan X, An Z, Wang X, Zhang D, Ono T (2018) Preparation of graphene-enhanced nickel-phosphorus composite films by ultrasonic-assisted electroless plating Appl. Surf Sci 435:617–625. https://doi.org/10.1016/j.apsusc.2017.11.169

26. Dong X, Zhou T, Pang S, Liang Z, Yu Q, Ruan B, Wang X (2019) Comparison of fly cutting and transverse planing for micropyramid array machining on nickel phosphorus plating. J Adv Manuf Technol, Int. https://doi.org/10.1007/s00170-019-03335-8

27. Dong X, Zhou T, Pang S, Liang Z, Yu Q, Ruan B, Wang X (2018) Defect analysis in microgroove machining of nickel-phosphide plating by small cross-angle microgrooving. J Nanomater 2018:1–9. https://doi.org/10.1155/2018/1478649

Tianxing Wang is a master candidate at Key Laboratory of Fundamental Science for Advanced Machining, Beijing institute of technology. His research interests include the functional surface with micro/nano structures.

Zhou Tianfeng is a professor of Beijing Institute of Technology and served as the deputy director of the Department of Manufacturing Engineering. He is doctoral tutor, young thousand and the chief scientist of young 973 program. His main research directions include mold materials preparation, mold manufacturing, glass molding, micro/nano manufacturing and so on. He has published more than 90 papers, including more than 50 SCI papers. He applied for more than 40 invention patens, and authorized more than 10 patents.

Xiaobin Dong received his Ph.D. degree in mechanical engineering from Beijing Institute of Technology. His research interests include the machining of micro/nano structures.

Peng Liu is a postdoctoral researcher at Beijing Institute of Technology, and his research directions include design and integration of optical systems, laser materials processing, numerical simulation, etc.

Yupeng He is a Ph.D. candidate at Key Laboratory of Fundamental Science for Advanced Machining, Beijing institute of technology. His research interests include the manufacturing and applications of micro/nano structures, especially the optical micro/nano structures.

Wenxiang Zhao is a professor at Key Laboratory of Fundamental Science for Advanced Machining, Beijing institute of technology. He mainly engages in the theoretical and technical research in the fields of high-efficiency precision cutting and grinding of difficult-to-machine materials.

Jiwang Yan is a professor of Keio University. His research directions include ultra-Precision machining, micro/nano manufacturing, laser processing of materials, glass molding/imprinting, nanoindentation physics, nano-material-based fabrication.

Yao Hu is an associate professor at Beijing Key Laboratory for Precision Optoelectronic Measurement Instrument and Technology, Beijing Institute of Technology. Her research interests include the interferometry, grating detection and application.